Base of brain intelligence: Information flow in cultured neuronal networks and its simulation on 2D mesh network

Shinichi Tamura[a,b,*], Yoshi Nishitani[b], Chie Hosokawa[c], Yuko Mizuno-Matsumoto[d], Yen-Wei Chen[e]

[a]*NBL Technovator Co., Ltd., 631 Shindachimakino, Sennan 590-0522, Japan*
[b]*Dept. of Radiology, Graduate School of Medicine, Osaka University, Suita 565-0871, Japan*
[c]*Health Research Institute, AIST, Ikeda, Osaka 563-8577, Japan*
[d]*Graduate School of Applied Informatics, University of Hyogo, Kobe 650-0047, Japan*
[e]*Graduate School of Science and Engineering, Ritsumeikan University, Kusatsu, 525-8577, Japan*
*Corresponding author: tamuras @ nblmt.jp

***Abstract*—It's important for understanding brain intelligence to investigate how the signal/ information is flown in neuronal network. We observed spike trains obtained by one-shot electrical stimulation with 8 × 8 multi-electrodes in cultured neuronal networks. Each electrode is considered to collect spikes from several neurons. We then constructed code flow maps as movies of the electrode array to observe the code flow especially of "1101" and "1011." To quantify the flow, we calculated the cross-correlations of the maximum direction of the codes with lengths less than 8. Normalized cross-correlations in the maximum direction were almost constant irrespective of code. Thus, the analysis suggested that the local codes for electrode flow maintained the code shape to some extent and conveyed information in the neural network. Then we made simulation of such code flow, and could estimate rough characteristics of neurons including refractory period and distribution of connection weights between neurons.**

Keywords—Cultured neural network, Spike train, Multi-electrode, Pseudo-random sequence, Code flow

I. INTRODUCTION

Spike trains can be observed in a neuronal network. They show various aspects of neurons when they fire. It is difficult, however, to determine how the spikes are coded. Furthermore, neurons work slowly and unreliably compared with artificial transistors, presenting a mystery of how a neuronal network can work intelligently and reliably.

The present methods of spike-coding analyses of neuronal networks are (A) spike-coding metrics, (B) spatiotemporal coding, (C) synchronous action model, and (D) pseudorandom code analysis [1]-[12].

From the viewpoint of the coding scheme of spike trains, we showed that M-sequence-related codes are detected significantly more often than those from time-shuffled trains [12]. These may contribute to communication between neurons from an analogy of artificial communication systems.

In this study, we first analyzed the spike trains of cultured neural networks by examining the code of a multielectrode array. Next, we visualized the flow of codes that were composed of spike sequences. We further quantified the flow of the codes that may reflect the flow of information in the neural network.

II. CODE SPECTRUM OF A CULTURED NEURAL NETWORK

The cell cultures of hippocampal neurons were dissected from 18-day-old Wistar rat embryos. Stimulated spikes that were produced by bipolar pulses (10 μA, 100 μs × 2) from one channel (electrode) were recorded by an extracellular recording system with 64 channels (MED64, Alpha MED Scientific Inc.) with a sampling frequency of 20 kHz. These procedures were basically the same as those described previously [12], [13]. Raster plots were obtained by detecting the peaks of recorded spike responses with a prespecified threshold (5 times the root mean square of4noise, peak-to-peak

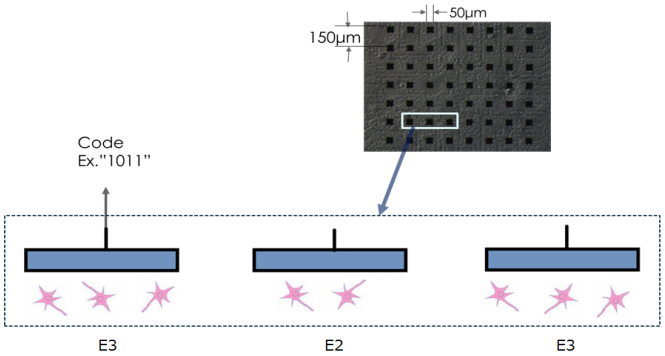

Fig. 1 (Upper) Micrograph of cultured hippocampal neurons in a microelectrode array. Black rectangles indicate electrodes. (Lower) Illustration of a vertical section. *E*3 means the electrode catches spikes of 3 neurons, and so on.

value) on each channel with a time bin width of 0.1 ms.

Because we did not sort the spikes, the spike train from each electrode may be composed of spikes from several neuronal cells as shown in Fig.1. From these spike trains, we confirmed that the M-sequence family occurred significantly more often than by chance [12]. In Fig. 2, we show the "1101" and "1011" detected codes of sample A as the simplest code pair with 1% nominal time accuracy on the 8 × 8 electrode arrangement up to 18 ms after the neurons were stimulated. Codes "1101" and "1011" are a core part of the reversal sequences "1101000" and "1011000" of the representative M-sequences of "0010111" and "0100111," respectively. Here, codes with bit width more than 0.6 ms are detected as shown in Fig.3.

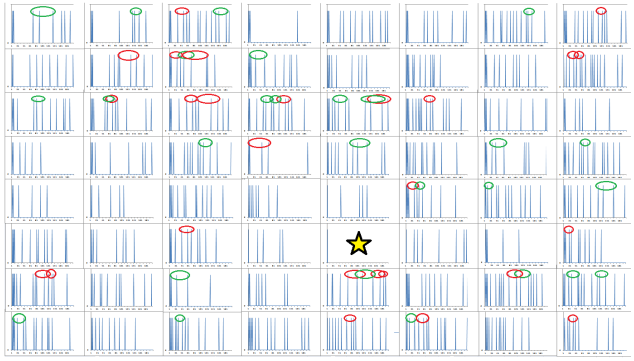

Fig.2 Spike trains on 8 × 8 multielectrodes between 0 and 18 ms (horizontal axis) after the stimulation pulse is given at time 0 from the electrode marked with a star. The red ellipse shows the code "1011," and the green ellipse shows "1101," with each having a bit width more than 0.6 ms.

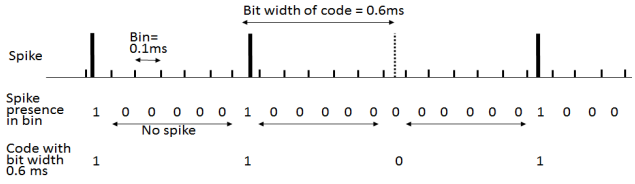

Fig.3 Code "1101" detected with bit width 0.6 ms

Fig. 4 shows a code spectrum from the 64 electrodes as an average of the 9 trials of sample A, in which the targeted and detected codes (sequences) were those having binary "1"s at both ends of the code and more than three "1"s, including both ends, with lengths less than 8 bits and the sequence between the terminal "1"s was an incremental binary number. Then, the order of the codes was sorted by the number of "1"s in the code. The total number of codes under investigation was 120. The length of the train data was 200 ms [2,000 data points/(electrode × trial)], which was sampled with a 0.1-ms bin-width, and the number of spikes ("1"s) on an electrode was an average per trial of 23.2 ± 9.1 in Sample A. The interval-shuffled trains (Shuf), the electrode-shuffled trains (EShuf) among 64 array electrodes, and randomly generated trains (Rand), in which six different trains were generated by a computer, were also analyzed. Roughly speaking, there were two such types of codes with high- and low-appearance rates divided between code nos. 21 and 22. The former were codes with three bits ("1"), including both end bits, whereas the latter were codes with four bits or more.

Code flow map of Sample A is shown as a movie in Fig.5.

Cross-correlation to the maximum direction $\Phi_N(C)$ that is normalized by the code length for 14 major codes of sample A is shown in Fig.6. 8N and 20N means that of between 8 and 20 neighbors, respectively, and the "maximum direction" means giving the maximum among 8N or 20N. This suggests that the local codes for electrode flow maintained the code shape to some extent and conveyed information in the neural network.

III. SIMULATION OF CODE GENERATION

We did simulation of generation of spike sequences from multi-electrode on 2D mesh type neural network with 31×31 neurons and weighted connections between 8 neighbor neurons. We set 8×8 electrodes on it, each of which gathers spikes from 2-9 neurons around it as shown in Fig.7.

The weight of the network is given by

$$w_{ij}=F[\,(1+a)u-a] \qquad i,j \in \{1, 2, \cdots, 31\},$$

where

$$F[x] = 1 \qquad 1 \leqq x$$
$$= x \qquad -1<x<1$$

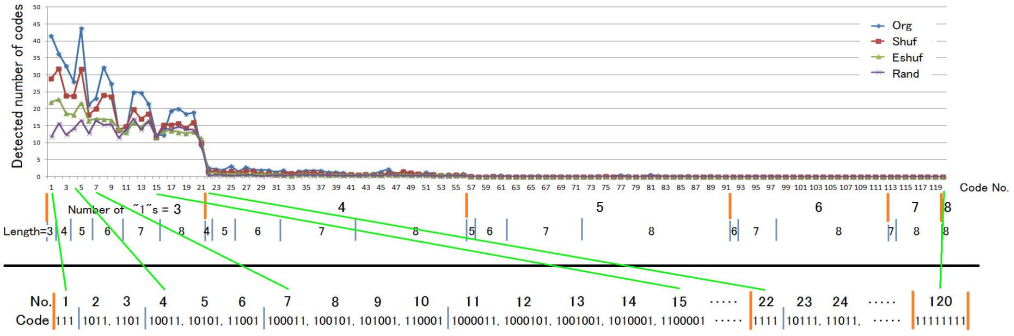

Fig.4 Spectrum of the detected codes with bit widths of 0.6–2.0 ms.

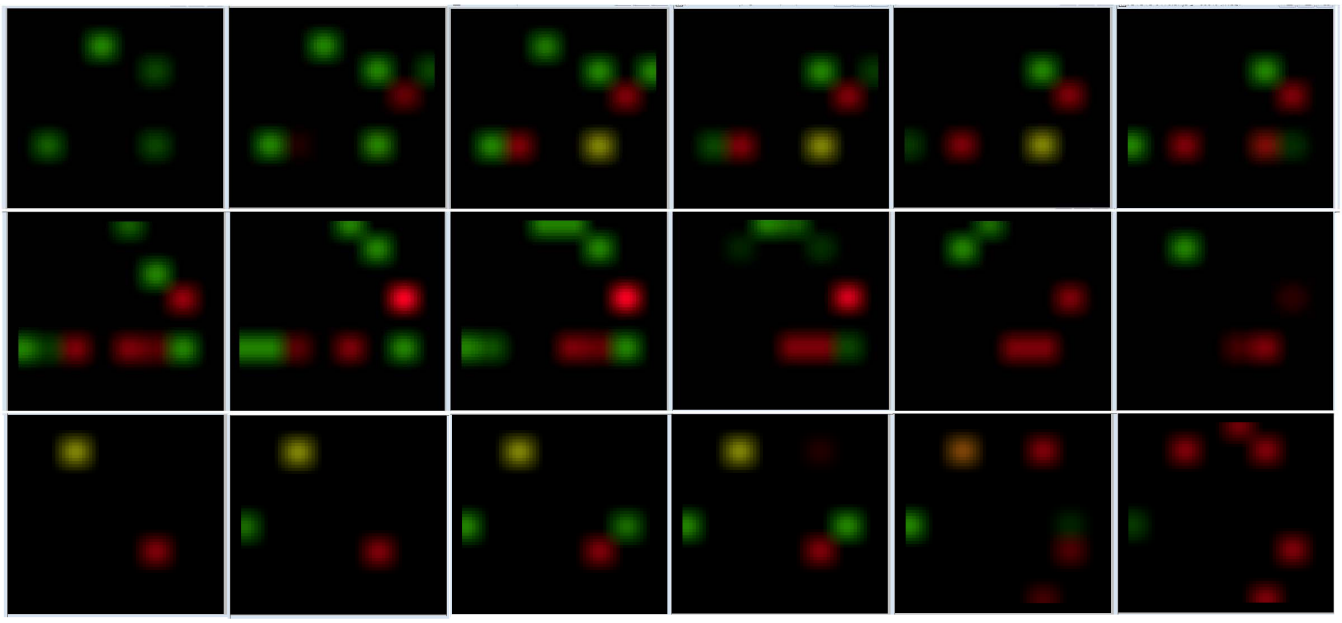

Fig.5 Code flow map of Sample B with bit width =0.6-3.0 ms. The serial images are from right to left and top to bottom, and the "1011" and "1101" codes are expressed in red and green, respectively. Yellow indicates a mixed code. These spots are blurred to smoothen the movies. The frame interval is 5 ms.

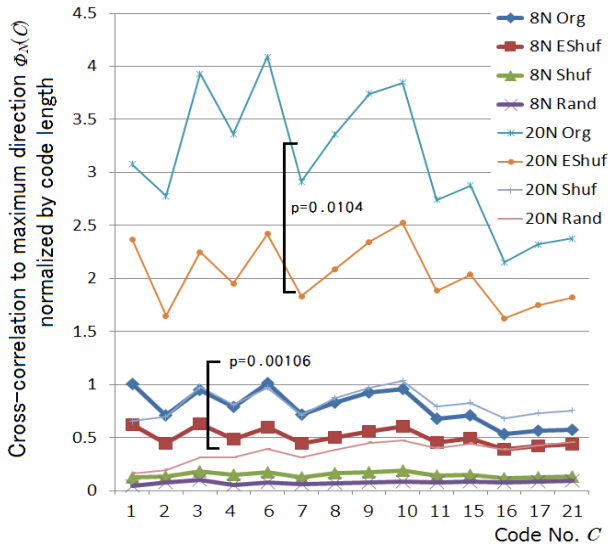

Fig. 6 Cross-correlation to the maximum direction $\Phi_N(C)$ that is normalized by the code length for 14 major codes of sample A. The p values are calculated from the EShuf/Org ratios of each code.

$= -1 \qquad x \leqq -1$

a = positive parameter such that $0 < a \leqq 3$
u = random variable with uniform distribution such that $0 \leqq u < 1$

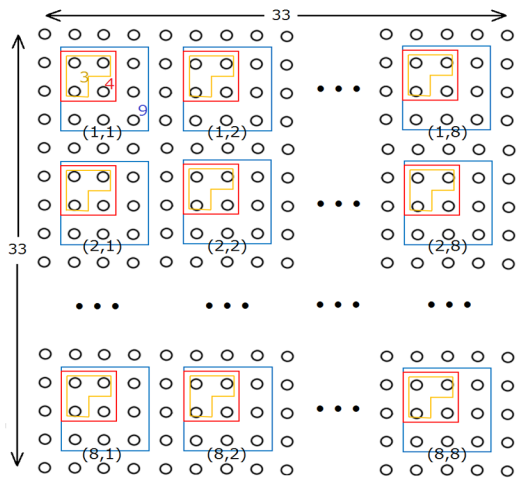

Fig.7 Arrangement of 8×8 multielectrode on simulated 2D mesh neural network. Each electrode catches spikes of 2-9 neurons. Connections between 8 neighboring neurons are generated randomly with some stochastic haracteristics.

By setting parameters of the simulation such as refractory period, connection weight distribution, and number of neuron cells whose spikes are collected by each electrode. These parameters are varied in each simulation as shown later. Further, there are another parameters of spontaneous fluctuations and fixed intrinsic transmission delay time and refractory period to each neuron cell. The variation of intrinsic

transmission delay time of each neuron cell is set one of {-3, -2, …, +3} with probability 1/7 each, where -3 corresponds -0.3ms and so on. That of refractory is set one of {-1, 0, +1} with probability 1/3 each. The spontaneous fluctuation of transmission delay time of each neuron cell is set {-1, 0, +1} with probability 1/12, 5/6, and 1/12, respectively, and that of refractory period is also set {-1, 0, +1} with probability 1/12, 5/6, and 1/12, respectively. These additional parameters are set fixed through the simulation in this paper.

Fig.8 shows, as an example, case of code spectrum of generated spike sequence in case of *Tref* (median of refractory period) = 7ms and connection weight parameter a=2. Practically, the number of neuron cells effecting each electrode changes by each electrode. Therefore, real observed code spectrum will be mixed according to the distribution of number of neuron cells (*En*) around electrodes.

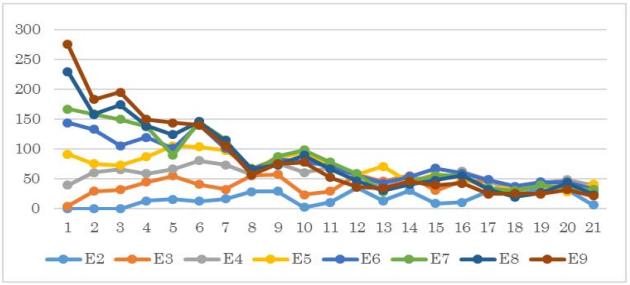

Fig. 8 Code spectrum of generated spike sequence in case of *Tref* (median of refractory period)=7ms and connection weight parameter a=2. Observed number of codes (Code No.1-21) from 64 electrodes between 200ms after stimulation, which is sampled with 0.1 ms time bin, that is composed of totally 2000 time bins. Bit length of code is 0.6-2.0ms. *E*2 means in case of each electrode catches spikes from 2 neuron cells, and so on.

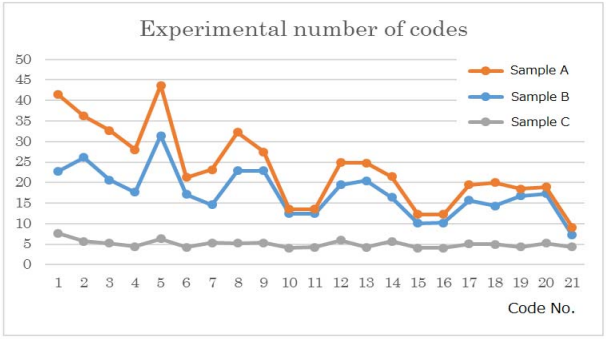

Fig. 9 Experimental number of codes detected in spike trains expressed with 2000 time bins of 0.1 ms for 3 Samples. Bit width of code is 0.6-2.0 ms (6-20 bins). Basically, codes are detected with 1 % of time accuracy, though practically several % because of 0.1 ms of bit width.

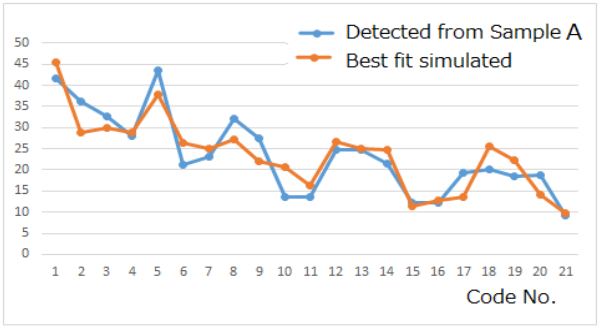

Fig. 10 Best fit to code Spectrum A by simulation spectrum set with *Tref*=6 ms and a=2.5. Distribution of *En* (n=2, 3, ⋯, 9) is (1/10, 1/2, 0, 1/20, 0, 0, 0, 7/20). Normalized RMS error is 0.179.

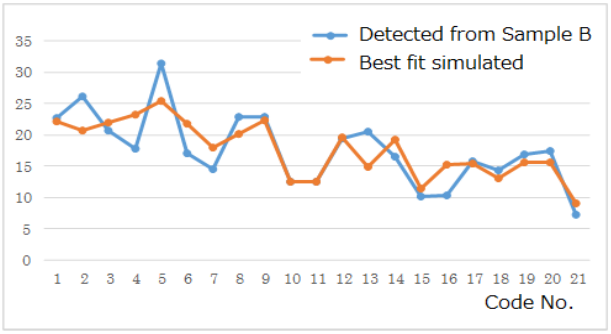

Fig. 11 Best fit to code Spectrum B by simulation spectrum set with *Tref*=7 ms and a=2. N Distribution of *En* (n=2, 3, ⋯, 9) is (3/10, 1/10, 0, 0, 0, 1/20, 0, 11/20). Normalized RMS error is 0.181.

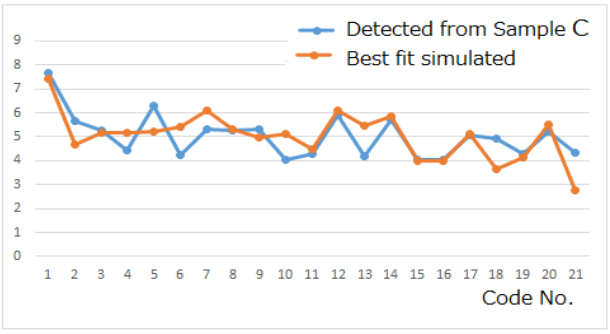

Fig.12 Best fit to code Spectrum C by simulation spectrum set with *Tref*=5 ms and a=3. Distribution of *En* (n=2, 3,⋯, 9) is (1/5, 1/5, 1/10, 0, 0, 0, 0, 1/2). Normalized RMS error is 0.149.

Fig.9 shows experimental results of detected average number of codes (1-21) from Sample A, B, and C.

Fig.10-12 show best fit to the number of codes detected in spike trains on 2000 time bins of Sample A, B, and C by code spectrums of artificially generated spike sequence with various

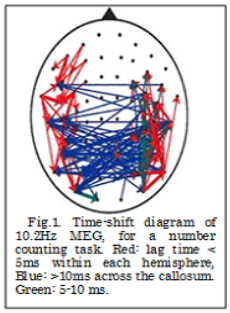

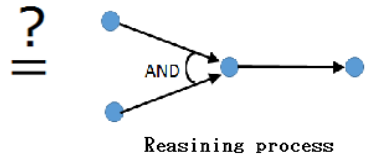

Fig.13 Does the time-shift map correspond to reasoning process?

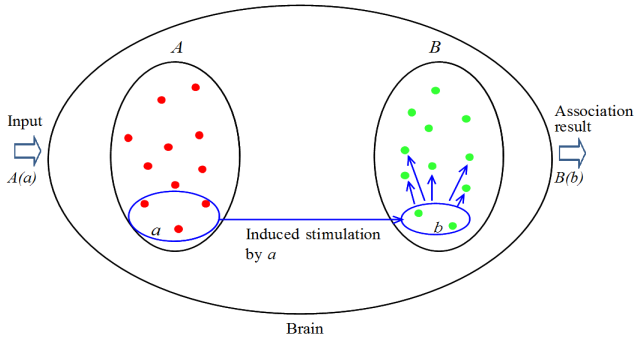

(a) Association process

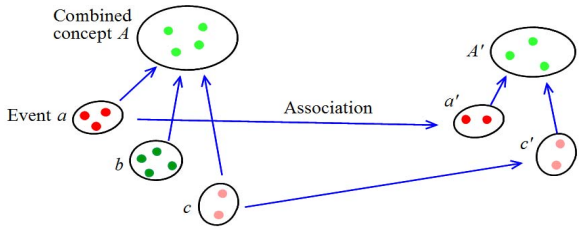

(b) Abstraction process

Fig.14 Higher order intelligence by communication or informaion flow by spike waves where the spike code is a part of them and made visible in this paper.

refractory period *Tref* and connection weight parameter *a*, and distribution of *En*. Since it is an inverse problem, and not perfect, estimation of neuronal these parameters of *Tref, a*, and *En* are possible to some extent.

IV. . Discussion and Conclusion

To date, the coding mechanisms of neural networks have not been solved.

We observed spike trains that were produced by one-shot electrical stimulation of neuronal networks cultured on 8 × 8 multielectrodes. Each electrode accepted spikes from several neurons. We extracted short codes from each electrode and obtained a code spectrum. These codes were considered to be composed of the neuron circuits around the corresponding electrode. However, some codes may be observed by chance. To clarify this, we constructed code flow maps as movies of the electrode array to observe the code flows of "1101" and "1011." They seemed to flow from electrode to neighboring electrode while keeping their shapes to some extent. We showed that if we shuffled the spike train interval, they became random with no flow.

To quantify the flow, we calculated the cross-correlations to the maximum direction of the codes with lengths less than 8. We found that the normalized cross-correlations were almost constant, irrespective of code. Furthermore, we showed that if we shuffled the spike trains in interval orders or in electrodes, they became significantly small.

Thus, the analysis suggested that the local codes around the electrode flow maintained the code shape to some extent, and they transported the information in the neural network. The short code may have been generated by local circuits, including feedback loops [12] or various transmission delays [11]. If so, the result will help estimate the local circuit shape. The analysis proposed here can also be regarded as the code decomposition of random-like spike trains with nonindependent components (codes).

The problem is that the observed code maps have no repeatability except for the statistical characteristics as treated here or within such short term as 20 ms where PSTH (poststimulus time histogram) can be observed with coherency between neighboring neurons. Although the period to which the repeatability is kept is 15 ms or so after stimulation [14], this short term coherency seems enough for such neuronal network where various information goes and forth. This issue will be discussed in another paper.

We have visualized information flow in brain by time-shift map from cross-correlation of MEG or EEG [15]. It can show up to small flow in the brain, and it may be reasonable to represent some aspects of logics in the brain as Fig.13. If this is the case, higher order brain intelligence process will be expressed as Fig.14. However, these are subjects to be attacked hereafter.

References

[1] Cessac, B., Paugam-Moisy, H., & Viéville, T. (2010). Overview of facts and issues about neural coding by spike. J. Physiol., Paris, 104, (1-2), 5-18.

[2] Kliper, O., Horn, D., Quenet, B., & Dror, G. (2004). Analysis of spatiotemporal patterns in a model of olfaction. Neurocomputing 5860, 1027-1032.

[3] Fujita, K., Kashimori, Y., & Kambara, T. (2007). Spatiotemporal burst coding for extracting features of spatiotemporally varying stimuli. Biol. Cybern., 97, 293-305. Doi: 10.1007/s00422-007-0175-z.

[4] Tyukin, I., Tyukina, T., & Leeuwen, C. van (2009). Invariant template matching in systems with spatiotemporal coding: A matter of instability. Neural Networks, 22, 425-449.

[5] Mohemmed, A., Schliebs, S., Matsuda, S., & Kasabov, N. (2013). Training spiking neural networks to associate spatio-temporal input–output spike patterns. Neurocomputing, 107, 3–10.

[6] Olshausen, B., & Field, D. (1996). Emergence of simple-cell receptive field properties by learning a sparse code for natural images. Letters to Nature 381, 607-609. [9] Abeles, M. (1982). Local Cortical Circuits: An Electrophysiological study. Springer, Berlin.

[7] Bell A., & Sejnowski, T. (1997). The independent components of natural scenes are edge filters. Vision Research, 37, 3327-3338.

[8] Tamura S., Mizuno-Matsumoto, Y., Chen, Y. W., & Nakamura, K. (2009). Association and abstraction on neural circuit loop and coding. The Fifth International Conference on Intelligent Information Hiding and Multimedia Signal Processing (IIHMSP2009) A10-07(No.546).

[9] Abeles, M. (1982). Local Cortical Circuits: An Electrophysiological study. Springer, Berlin.

[10] Abeles, M. (2009). Synfire chains. Scholarpedia, 4(7), 1441.

[11] Izhikevich, E. M. (2006). Polychronization: Computation with spikes. Neural Computation, 18, 245-282.

[12] Nishitani, Y., Hosokawa, C., Mizuno-Matsumoto, Y., Miyoshi, T., Sawai, H., & Tamura, S. (2012). Detection of M-Sequences from Spike Sequence in Neuronal Networks. Computational Intelligence and Neuroscience, vol. 2012, Article ID 862579, 9 pages. doi:10.1155/2012/862579.

[13] Hosokawa, C., Kudoh, S. N., Kiyohara, A., & Taguchi, T. (2008). Resynchronization in neuronal network divided by femtosecond laser processing. Neuroreport, 19, 771-775.

[14] Baljon, P. L., Chiappalone, M., & Martinoia. (2009). Interaction of electrically evoked responses in networks of dissociated cortical neurons. Physical Review, E 80, 031906-(1-10).

[15] Mizuno-Matsumoto Y., Okazaki K., Kato A., Yoshimine T., Sato Y., Tamura S., and Hayakawa T.: Visualization of epileptogenic phenomena using crosscorrelation analysis: Localization of epileptic foci and propagation of epileptiform discharges. *IEEE Trans. Biomed. Eng.,* vol.46, No.3, 271-9, 1999.